

## Article

# Fluorescence Detecting of Paraquat and Diquat Using Host–Guest Chemistry with a Fluorophore-Pendant Calix[6]arene

 Ermanno Vasca <sup>1</sup>, Francesco Siano <sup>2</sup> and Tonino Caruso <sup>1,\*</sup>
<sup>1</sup> Department of Chemistry and Biology, University of Salerno, 84084 Fisciano, Italy

<sup>2</sup> Institute of Food Science, National Research Council, 83100 Avellino, Italy

\* Correspondence: tcaruso@unisa.it

**Abstract:** Paraquat (PQ) and diquat (DQ), some of the most widely used herbicides in the world, both present a high mortality index after intentional exposure. In this paper, a fluorescence sensing method for PQ and DQ, based on host–guest molecular recognition, is proposed. Calix[6]arene derivatives containing anthracene or naphthalene as pendant fluorophore at their lower rim recognize DQ and PQ in hydroalcoholic solution with a broad linear response range at the  $\mu\text{g L}^{-1}$  level concentration. The linear response ranges were found from 1.0 to 18  $\mu\text{g L}^{-1}$  with the detection limit of 31  $\text{ng L}^{-1}$  for paraquat, and from 1.0 to 44  $\mu\text{g L}^{-1}$  with the detection limit of 0.16  $\mu\text{g L}^{-1}$  for diquat. The recognition process is detected by following the decrease in the fluorescence emission consequent to complexation. The proposed quenching method has been applied to the determination of paraquat in drinking water samples.

**Keywords:** fluorescence quenching; herbicides; paraquat; diquat; molecular recognition



**Citation:** Vasca, E.; Siano, F.; Caruso, T. Fluorescence Detecting of Paraquat and Diquat Using Host–Guest Chemistry with a Fluorophore-Pendant Calix[6]arene. *Sensors* **2023**, *23*, 1120. <https://doi.org/10.3390/s23031120>

Academic Editor: Vittorio Passaro

Received: 16 December 2022

Revised: 11 January 2023

Accepted: 16 January 2023

Published: 18 January 2023



**Copyright:** © 2023 by the authors. Licensee MDPI, Basel, Switzerland. This article is an open access article distributed under the terms and conditions of the Creative Commons Attribution (CC BY) license (<https://creativecommons.org/licenses/by/4.0/>).

## 1. Introduction

Paraquat (1,1'-dimethyl-4,4'-bipyridylium dichloride, PQ) and diquat (1,1'-ethylene-2,2'-bipyridylium dibromide, DQ) (Figure 1) are non-selective and nonsystematic contact herbicides widely used in agriculture to control broadleaf and grassy weeds. The use of these herbicides is important because weeds compete vigorously with crops for water, light and other nutrients. However, both contain a diquaternary bipyridyl unit that is responsible for their herbicidal and toxicological properties, while the halogen anions have few toxic effects [1–3]. Because of their highly toxic effects on humans, their use is “restricted” in the USA and banned in the EU and elsewhere [4–6].



**Figure 1.** (a) Paraquat dichloride, PQ. (b) Diquat dibromide, DQ.

The detection and quantitative determination of bipyridilium herbicides are somewhat difficult mainly because they are cationic molecules. As in the case of quaternary amines, for chromatography and hyphenated techniques [7–11], their inherent high polarity and positive charge make it necessary to use ion pairing additives if reversed-phase columns are used. Numerous other methods have been developed to monitor and control these herbicides in the environment, water, food and clinical samples, including capillary electrophoresis [12], voltammetry [13,14] and immunoassay [15,16]. Fluorescence spectroscopy is known for its sensitivity, high specificity, selectivity, speed, simplicity and low cost as

compared to other analytical techniques [17]. Due to the high levels of sensitivity and particularly their ability to be used for temporal and spatial sampling for *in vivo* imaging applications, fluorescent chemosensors based on molecular recognition have been widely applied in a variety of fields such as biology, physiology, pharmacology and environmental sciences [18,19]. Variations in the fluorescence spectrum of a guest molecule (G), consequent to complexation, are usually used to detect trace amounts of a host analyte (H).

However, few fluorescence methods have been developed for paraquat and diquat detection [20–24]. Recently, a novel non-covalently linked photoreactive dyad was synthesized by applying supramolecular assembly based on a calixarene host–guest chemistry [25], in which the fluorescent probes, naphthalene or anthracene, are covalently attached to the host (Figure 2).

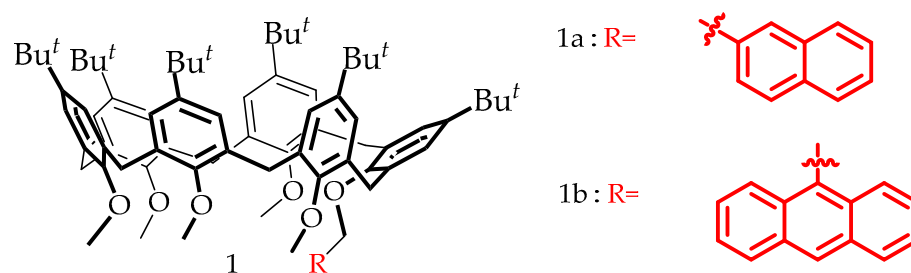


**Figure 2.** Calix[6]arene hosts 1a and 1b with fluorophores covalently linked.

Naphthalene and anthracene are indeed the most widely used fluorogenic units in the synthesis of fluorescent calixarene host [26–28]. It was demonstrated that simple calixarenes can be efficient wheels toward dialkylammonium axles by exploiting the inducing effect of the weakly coordinating tetrakis[3,5-bis-(trifluoromethyl)phenyl]borate (TFPB<sup>-</sup>) [29]. Threading of calix[6]arene macrocycles to the TFPB salt of dialkylammonium cations can be a valid tool to prepare a fluorescent pseudo-rotaxane, a host–guest system composed minimally of a threadlike molecule “as axles” surrounded by a macrocycle [30].

Based on this strategy, diquat dibromide (DQ) and paraquat dichloride (PQ) are expected to behave similarly to the dialkylammonium axles. In the present study, the chemosensory behavior of these pseudo-rotaxanes composed by a new calixarene hosts with paraquat and diquat was investigated by fluorescence spectroscopy, in order to develop a sensitive fluorescent detection method for PQ and DQ in water samples.

## 2. Materials and Methods

All solvents used in this study for fluorescence measurements were of spectrophotometric grade. Chloroform, methanol and deionized water were purchased from Sigma-Aldrich Corporation. All reagents used in this study were of analytical grade. Diquat dibromide monohydrate (DQ), paraquat dichloride hydrate (PQ) and the interfering species investigated in this work, carbaryl, atrazine and triclopyr, all were purchased from Sigma-Aldrich. Anion and cations were prepared from ionic salts (NaCl, KNO<sub>3</sub>, Na<sub>2</sub>CO<sub>3</sub>, Na<sub>2</sub>SO<sub>4</sub>, Na<sub>3</sub>PO<sub>4</sub>, MgCl<sub>2</sub>, CaCO<sub>3</sub> and ZnSO<sub>4</sub>·7H<sub>2</sub>O) purchased from Merck. The calixarene hosts 1a and 1b (Figure 2) used in this study were synthesized and purified by HPLC by a published method [25,31].

To investigate the complexing ability of 1a and 1b toward DQ and PQ dications, fluorometric titration experiments were performed. The association constants of 1a and 1b with PQ and DQ cannot be determined by UV–Vis spectroscopy, because spectral changes upon host–guest interaction are too small. The chemosensor behavior of the new host with PQ and DQ was investigated by fluorescence spectroscopy in a chloroform–methanol 1:1 solvent mixture. UV–Vis spectra were recorded on a Varian Cary 50 UV–Vis Spectrophotometer, in the 200–800 nm wavelength interval, to determine the maximum of the absorption spectrum of the fluorophores 1a and 1b. This allowed us to select the excitation frequency for the successive fluorescence experiments, according to Kasha’s rule [32].

The most intense spectra were obtained with an excitation energy slightly higher than the one corresponding to the absorption maximum (ca 50 eV). Fluorescence measurements were performed on a Varian Cary Eclipse Fluorescence Spectrophotometer equipped with a Varian Cary Single Cell Peltier to conduct measurements at a controlled temperature. A Thermo Scientific UltiMate 3000 Binary semi-preparative system, equipped with an Agilent RP Prep-C18 Scalar column, 100 Å, 4.6 mm × 150 mm, 10 µm and a Diode array detector, was used for purifying the host compounds [31]. A Metrohm 787 KF Titrino Karl Fisher Titration System was used to determine the water content in the solid samples [33]. A Metrohm 715 Dosimat was used to dose a titration solution with the precision of ±0.001 mL. A Mettler Toledo XS105DR analytical balance was used to weigh with a precision of ±0.01 mg. To value if the herbicide concentration depends on the matrix of the sample, a Perkin-Elmer ICP-OES Optima 3000 Dual View Spectrophotometer was used to determine the metal concentration in a tap water sample, and Thermo-Dionex Aquion Ion Chromatography was used to determine the anion concentration in a tested tap water sample.

### 3. Results and Discussion

#### 3.1. Determination of Association Constants by Fluorometric Titration

The most common approach for quantifying interactions in supramolecular chemistry is a guest–host titration, noting the changes in some physical property through NMR, UV–Vis, fluorescence or other techniques. For this purpose, to avoid the volume variation, H-G solutions were prepared by adding equal volumes of the solutions with the same host concentration to different volumes of the paraquat or diquat standard solution. The final volume of each solution was made up to the same total volume by fixing with the solvent mixture. All the solutions were prepared in chloroform–methanol 1:1 mixture solution, equilibrated in a sealed vial at 25 °C for 24 h before measurements. The experimental values are reported in Tables 1–4.

**Table 1.** Experimental data for the determination of spectra reported in Figure 3. The  $V_{1a}$  and  $V_{PQ}$  volumes refer to an initial 1a solution with a concentration of 45.5 µg L<sup>-1</sup> and paraquat, PQ, solution with a concentration of 1000 µg L<sup>-1</sup>, respectively. The final volume of each solution was made up to a total volume of 3000 µL by fixing with the solvent mixture.

Entry	$V_{1a}$ , µL	$V_{PQ}$ , µL	$V_{TOT}$ , µL	[1a], µg L <sup>-1</sup>	[PQ], µg L <sup>-1</sup>	PQ/1a, mol/mol
1	2000	0	3000	30.3	0.0	0.0
2	2000	2	3000	30.3	0.7	0.1
3	2000	4	3000	30.3	1.3	0.2
4	2000	7	3000	30.3	2.3	0.4
5	2000	11	3000	30.3	3.7	0.6
6	2000	16	3000	30.3	5.3	0.8
7	2000	20	3000	30.3	6.7	1.0
8	2000	27	3000	30.3	9.0	1.4
9	2000	35	3000	30.3	11.7	1.8
10	2000	45	3000	30.3	15.0	2.3
11	2000	53	3000	30.3	17.7	2.7
12	2000	65	3000	30.3	21.7	3.3
13	2000	75	3000	30.3	25.0	3.8
14	2000	92	3000	30.3	30.7	4.7
15	2000	105	3000	30.3	35.0	5.3
16	2000	115	3000	30.3	38.3	5.8
17	2000	132	3000	30.3	44.0	6.7
18	2000	152	3000	30.3	50.7	7.7
19	2000	192	3000	30.3	64.0	9.7
20	2000	252	3000	30.3	84.0	12.7
21	2000	332	3000	30.3	110.7	16.8
22	2000	432	3000	30.3	144.0	21.8
23	2000	572	3000	30.3	190.7	28.9
24	2000	772	3000	30.3	257.3	39.0
25	2000	932	3000	30.3	310.7	47.1

**Table 2.** Experimental data for the determination of spectra reported in Figure 4. The  $V_{1b}$  and  $V_{PQ}$  volumes refer to an initial 1b solution with a concentration of  $50.7 \mu\text{g L}^{-1}$  and paraquat, PQ, solution with a concentration of  $1000 \mu\text{g L}^{-1}$ , respectively. The final volume of each solution was made up to a total volume of  $4000 \mu\text{L}$  by fixing with the solvent mixture.

Entry	$V_{1b}$ , $\mu\text{L}$	$V_{PQ}$ , $\mu\text{L}$	$V_{TOT}$ , $\mu\text{L}$	[1b], $\mu\text{g L}^{-1}$	[PQ], $\mu\text{g L}^{-1}$	PQ/1b, mol/mol
1	2000	0	4000	25.4	0.0	0.0
2	2000	3	4000	25.4	0.8	0.1
3	2000	6	4000	25.4	1.5	0.3
4	2000	9	4000	25.4	2.3	0.4
5	2000	12	4000	25.4	3.0	0.6
6	2000	16	4000	25.4	4.0	0.8
7	2000	20	4000	25.4	5.0	0.9
8	2000	25	4000	25.4	6.3	1.2
9	2000	32	4000	25.4	8.0	1.5
10	2000	40	4000	25.4	10.0	1.9
11	2000	50	4000	25.4	12.5	2.4
12	2000	60	4000	25.4	15.0	2.8
13	2000	75	4000	25.4	18.8	3.5
14	2000	90	4000	25.4	22.5	4.3
15	2000	110	4000	25.4	27.5	5.2
16	2000	135	4000	25.4	33.8	6.4
17	2000	155	4000	25.4	38.8	7.3
18	2000	185	4000	25.4	46.3	8.7
19	2000	225	4000	25.4	56.3	10.6
20	2000	285	4000	25.4	71.3	13.5
21	2000	365	4000	25.4	91.3	17.3
22	2000	464	4000	25.4	116.0	21.9
23	2000	650	4000	25.4	162.5	30.7
24	2000	800	4000	25.4	200.0	37.8
25	2000	1000	4000	25.4	250.0	47.3

**Table 3.** Experimental data for the determination of spectra reported in Figure 5. The  $V_{1a}$  and  $V_{DQ}$  volumes refer to an initial 1a solution with a concentration of  $45.5 \mu\text{g L}^{-1}$  and diquat, DQ, solution with a concentration of  $1650 \mu\text{g L}^{-1}$ , respectively. The final volume of each solution was made up to a total volume of  $3000 \mu\text{L}$  by fixing with the solvent mixture.

Entry	$V_{1a}$ , $\mu\text{L}$	$V_{DQ}$ , $\mu\text{L}$	$V_{TOT}$ , $\mu\text{L}$	[1a], $\mu\text{g L}^{-1}$	[DQ], $\mu\text{g L}^{-1}$	DQ/1a, mol/mol
1	2000	0	3000	30.3	0.0	0.0
2	2000	10	3000	30.3	5.5	0.6
3	2000	30	3000	30.3	16.5	1.9
4	2000	50	3000	30.3	27.5	3.1
5	2000	80	3000	30.3	44.0	5.0
6	2000	100	3000	30.3	66.0	7.5
7	2000	120	3000	30.3	66.0	7.5
8	2000	170	3000	30.3	93.5	10.6
9	2000	230	3000	30.3	126.5	14.3
10	2000	300	3000	30.3	165.0	18.7
11	2000	380	3000	30.3	209.0	23.7
12	2000	470	3000	30.3	258.5	29.3
13	2000	570	3000	30.3	313.5	35.5
14	2000	660	3000	30.3	363.0	41.1
15	2000	780	3000	30.3	429.0	48.6
16	2000	870	3000	30.3	478.5	54.2
17	2000	950	3000	30.3	522.5	59.2
18	2000	1000	3000	30.3	550.0	62.3

**Table 4.** Experimental data for the determination of spectra reported in Figure 6. The  $V_{1b}$  and  $V_{DQ}$  volumes refer to an initial 1b solution with a concentration of  $50.7 \mu\text{g L}^{-1}$  and diquat, DQ, solution with a concentration of  $1650 \mu\text{g L}^{-1}$ , respectively. The final volume of each solution was made up to a total volume of  $4000 \mu\text{L}$  by fixing with the solvent mixture.

Entry	$V_{1b}$ , $\mu\text{L}$	$V_{DQ}$ , $\mu\text{L}$	$V_{TOT}$ , $\mu\text{L}$	[1b], $\mu\text{g L}^{-1}$	[DQ], $\mu\text{g L}^{-1}$	DQ/1b, mol/mol
1	2000	0	4000	25.4	0.0	0.0
2	2000	2	4000	25.4	0.8	0.1
3	2000	5	4000	25.4	2.1	0.3
4	2000	9	4000	25.4	3.7	0.5
5	2000	14	4000	25.4	5.8	0.8
6	2000	20	4000	25.4	8.3	1.2
7	2000	28	4000	25.4	11.6	1.6
8	2000	39	4000	25.4	16.1	2.3
9	2000	54	4000	25.4	22.3	3.1
10	2000	74	4000	25.4	30.5	4.3
11	2000	104	4000	25.4	42.9	6.1
12	2000	144	4000	25.4	59.4	8.4
13	2000	204	4000	25.4	84.2	11.9
14	2000	284	4000	25.4	117.2	16.6
15	2000	384	4000	25.4	158.4	22.4
16	2000	504	4000	25.4	207.9	29.4
17	2000	654	4000	25.4	269.8	38.1
18	2000	854	4000	25.4	352.3	49.8
19	2000	1254	4000	25.4	517.3	73.1
20	2000	1574	4000	25.4	649.3	91.8

The emission spectra were recorded using excitation wavelengths of 285 nm for 1a and 263 nm for 1b, characteristic wavelengths of maximum absorption for the appended naphthalene or anthracene chromophore [34,35]. The addition of a highly concentrated chloroform–methanol solution of paraquat or diquat to a chloroform–methanol solution of the 1a or 1b host resulted in a drastic decrease in the intensity of the host emission peak (Figures 3 and 4). Similar results were observed in the diquat titration (Figures 5 and 6).

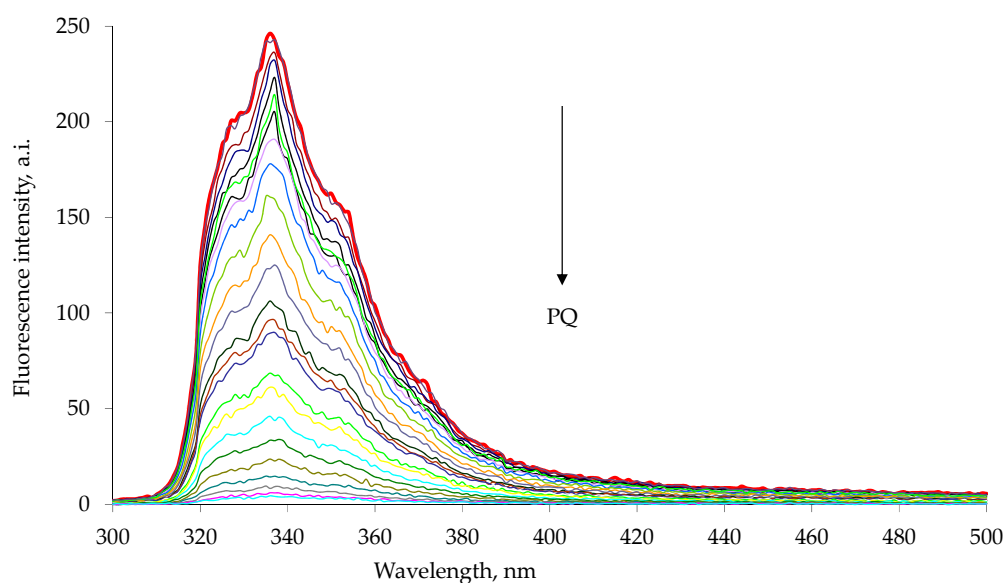


**Figure 3.** Fluorescence quenching of 1a host with increasing paraquat concentration, PQ, in chloroform–methanol 1:1 solution at  $25 \text{ }^\circ\text{C}$ . The experimental data are reported in Table 1. The emission spectra were measured with excitation at 285 nm. Each spectrum is reported with different color line (Entry 1–25 Table 1).

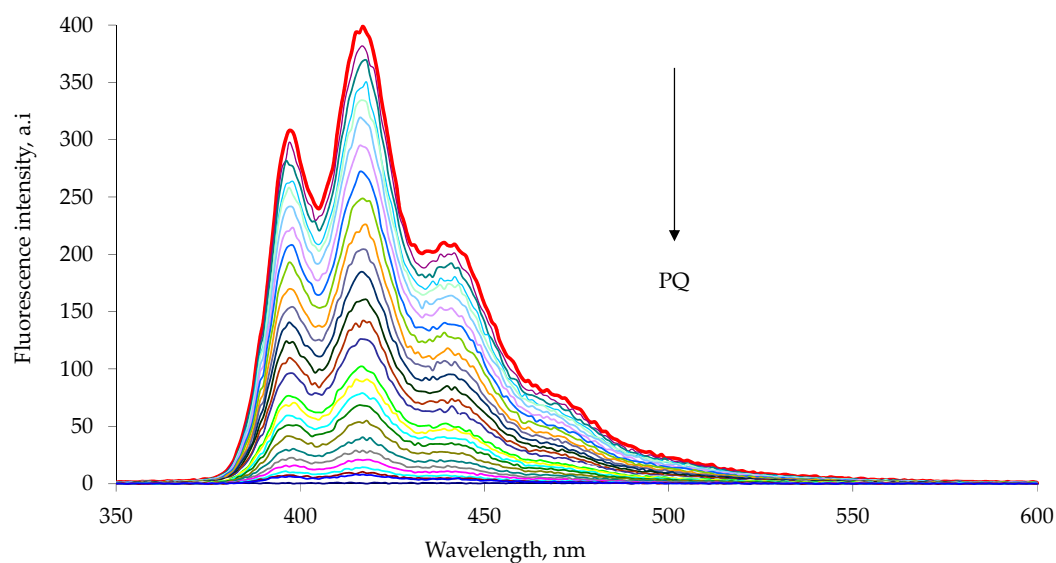


**Figure 4.** Fluorescence quenching of 1b host with increasing paraquat concentration, PQ, in chloroform–methanol 1:1 solution at 25 °C. The experimental data are reported in Table 2. The emission spectra were measured with excitation at 263 nm. Each spectrum is reported with different color line (Entry 1–25 Table 2).

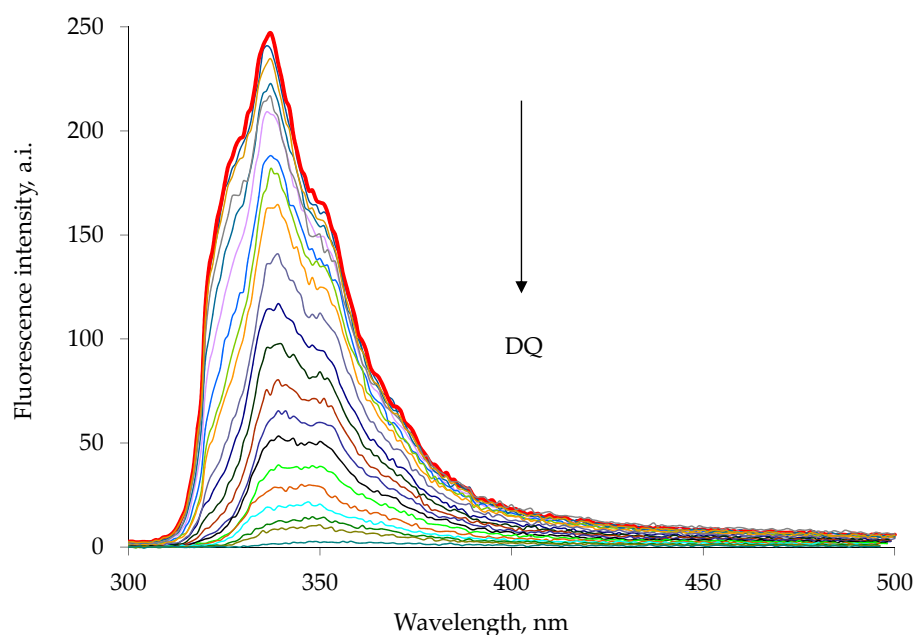


**Figure 5.** Fluorescence quenching of 1a host with increasing diquat concentration, DQ, in chloroform–methanol 1:1 solution at 25 °C. The emission spectra were measured with excitation at 285 nm. Each spectrum is reported with different color line (Entry 1–18 Table 3).

Based on the fluorescence measurements, the extended Benesi–Hildebrand equation (Equation (1)) can be used to calculate the association constants ( $K$ ) for the 1:1 model, considering that under the experimental conditions employed, the final concentration of the guest herbicide is much larger than that of the calixarene host, i.e.,  $[G] \gg [H]$  [36,37]. In this equation,  $\Delta F$  denotes the changes in the fluorescence intensity as  $F_0 - F$ , in which  $F_0$  is the value of the maximum fluorescence spectrum of the host, and  $\Delta \epsilon$  denotes the molar extinction coefficient of the H-G complex.

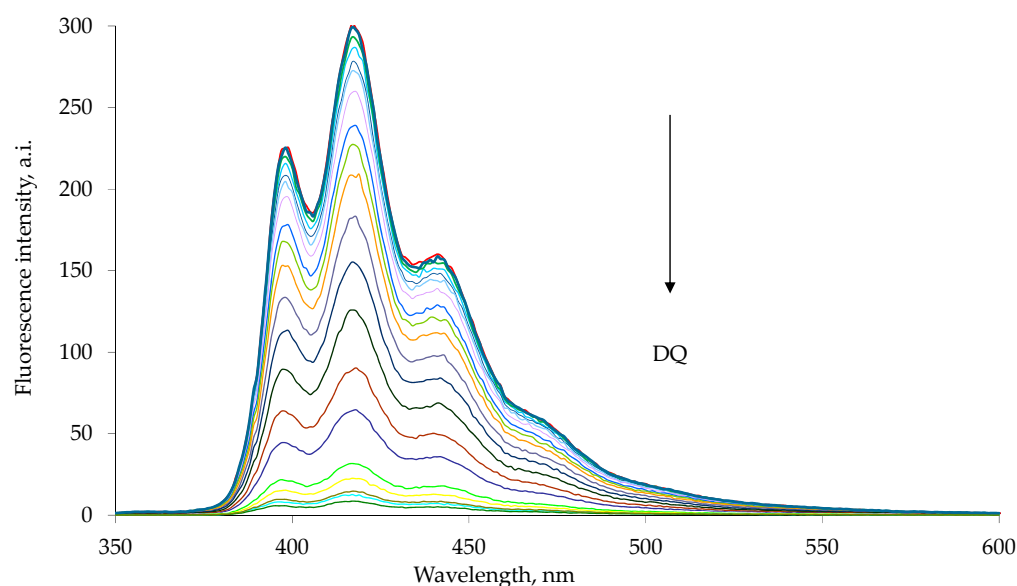


**Figure 6.** Fluorescence quenching of 1b host with increasing diquat concentration in chloroform–methanol 1:1 solution at 25 °C. The emission spectra were measured with excitation at 263 nm. Each spectrum is reported with different color line (Entry 1–20 Table 4).

$$\frac{[H][G]}{[\Delta F]} = \frac{1}{K\Delta\epsilon} + \frac{[G]}{\Delta\epsilon}, \quad (1)$$

Figure 7 illustrates the results of such a treatment for the H-G interaction, where the calculated values of  $[H][G]/[\Delta F]$  are reported against the molar concentrations of G, affording an adequate linear relationship.

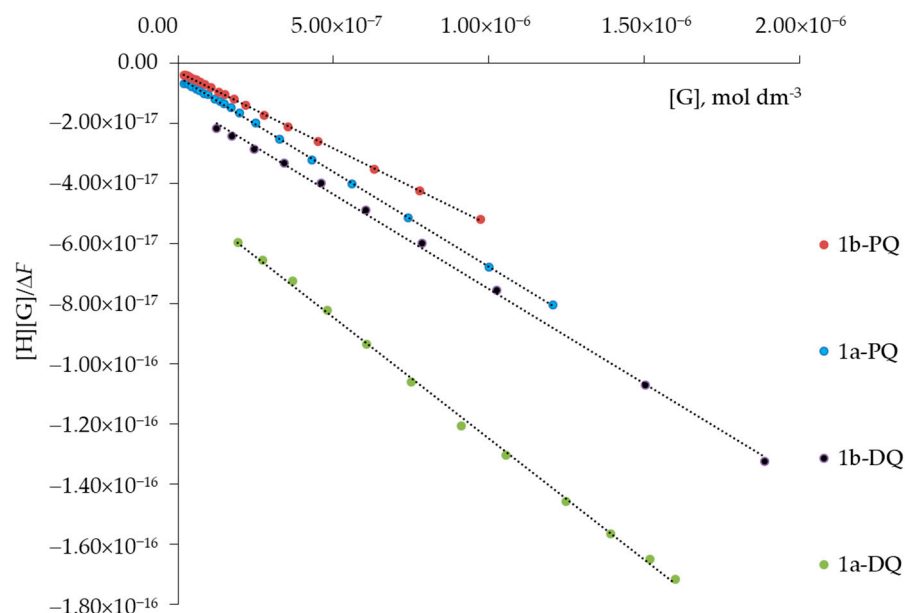


**Figure 7.** Typical plot of  $[H][G]/\Delta F$  versus  $[G]$ , mol dm<sup>-3</sup> for the complexation of host 1a (or 1b) with the guest (G), paraquat (PQ) or diquat (DQ). The dashed lines represent the fitted function by using Equation (1).

The values of the constants for the 1:1 complex calculated from the slope and intercept of  $[H][G]/\Delta F$  versus  $[G]$  plots are reported in Table 5.

**Table 5.** Association constants of H-G complexes at 25 °C, reported as log*K*. Paraquat, PQ, and diquat, DQ, are the guests, G, and the compounds 1a and 1b are the fluorescent hosts, H. The values were determined by Equation (1). Uncertainties are given as standard deviation.

Guest	Host	
	1a	1b
DQ	6.3 ± 0.3	6.7 ± 0.1
PQ	7.1 ± 0.1	7.3 ± 0.1

The binding constant 1:1 of PQ–host is higher than that of DQ–host probably due to the planar structure of PQ compared to DQ. Calculations are being made to determine the interaction energy between the aromatic units of calix and herbicide guests, as in the case of stacking interactions between two nucleobases [38]. Moreover, the fit of the experimental data with non-linear least squares was found to be independent of the  $K_{12}$  value. Therefore, the 1:1 model prevails [39].

### 3.2. Stern–Volmer Plot

Fluorescence quenching refers to any process that decreases the fluorescence intensity of the sample. A variety of molecular interactions can result in quenching, such as excited-state reactions, molecular rearrangements, energy transfer, ground-state complex formation and collisional quenching. The quenching resulting from collisional encounters between the fluorophore and quencher is called collisional or dynamic quenching. The quenching resulting from a non-fluorescent complex formation between the fluorophore and the quencher is called static quenching. Both static and dynamic quenching require molecular contact between the fluorophore and quencher. Collisional quenching of fluorescence is described by the Stern–Volmer Equation (2):

$$\frac{F_0}{F} = 1 + K_D[Q], \quad (2)$$

In Equation (2),  $F_0$  and  $F$  are the fluorescence intensities in the absence and presence of quencher, respectively, and  $[Q]$  is the concentration of quencher, i.e., paraquat or diquat in this work.  $K_D$  is the Stern–Volmer quenching constant that depends on a bimolecular quenching constant and the lifetime of the fluorophore in the absence of quencher. It is important to recognize that the observation of a linear Stern–Volmer plot does not prove that collisional quenching of fluorescence has occurred.

The static quenching also results in linear Stern–Volmer plots, as described by the Stern–Volmer Equation (3):

$$\frac{F_0}{F} = 1 + K_S[Q], \quad (3)$$

The linear dependence of  $F_0/F$  on  $[Q]$  is identical to that observed for dynamic quenching, except that the static quenching constant  $K_S$  now coincides with the association constant H-G [35].

The Stern–Volmer plot of  $F_0/F$  versus  $[Q]$  is shown in Figure 8, for paraquat or diquat as the quencher. The ratios  $F_0/F$  display a pronounced upward curvature at high concentrations of the quencher. This characteristic feature of the Stern–Volmer plot is typical for quenching that results both by collisions and by complex formation with the same quencher [35,40–42]. A modified form of the Stern–Volmer Equation (4) accounts for the upward curvature observed when both static and dynamic quenching occur for the same fluorophore [35] (pp. 282–284):

$$\frac{F_0}{F} = (1 + K_D[Q]) \cdot (1 + K_S[Q]), \quad (4)$$

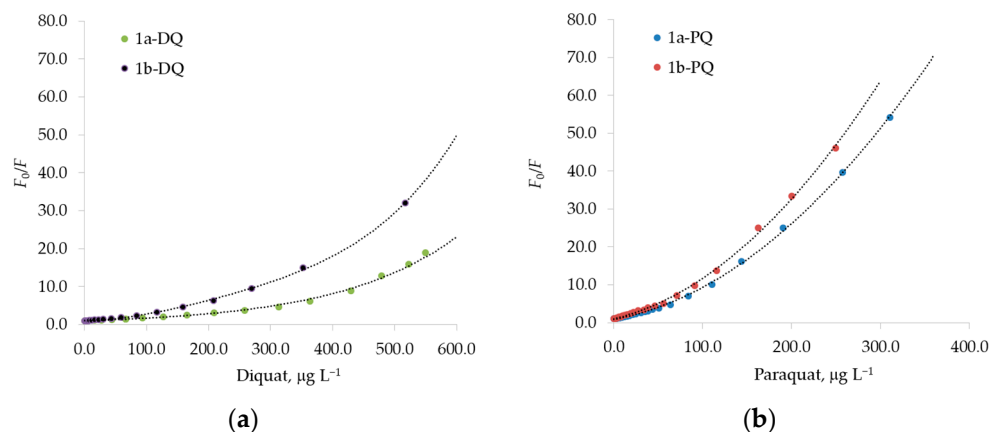


**Figure 8.** A modified Stern–Volmer plot of  $F_0/F$  against increasing concentration of quencher guests. (a) The experimental behavior for the diquat, DQ, as quencher of 1a and 1b fluorophores. (b) The experimental behavior for the paraquat, PQ, as quencher of 1a and 1b fluorophores. The dashed lines represent the curvature provided by Equation (4). The excitation wavelength was set to 285 nm and 263 nm, and the fluorescence value  $F$  was measured at 336 nm and 416 nm for the fluorophores 1a and 1b, respectively.  $F_0$  is the fluorescence intensity in the absence of quencher PQ or DQ.

Moreover, we also observed strict linearity of the  $F_0/F$  Stern–Volmer plot until 60 and 90  $\mu\text{g L}^{-1}$  for paraquat and diquat, respectively, as reported in Figure 9. As discussed above, when the Stern–Volmer plot is linear, only one type of quenching occurs, probably a static quenching. Indeed, by using Equation (3), the values for the H–G binding constants can be calculated [35]. These values (see Table 6) are similar to the those determined by fitting the spectral data according to the Benesi–Hildebrand equation (Figure 7, Table 5) [39]. Therefore, dynamic quenching is negligible at a low guest concentration [35] (p. 282), when the formation of the strong 1:1 complex prevails.

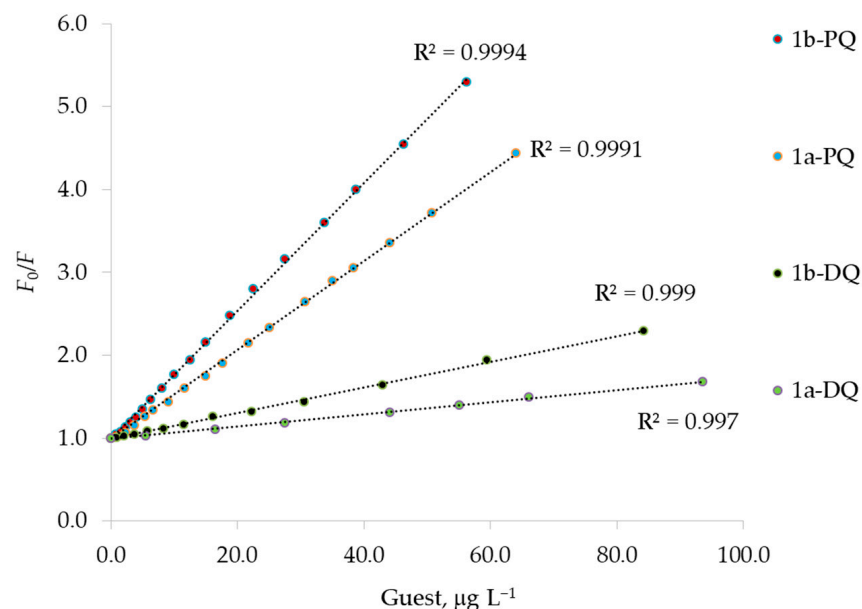


**Figure 9.** Stern–Volmer plots for the fluorescence quenching of 1a and 1b host with paraquat, PQ, and diquat, DQ, as guests. The excitation wavelength was set to 285 nm and 263 nm, and the fluorescence value  $F$  was measured at 336 nm and 416 nm for the fluorophores 1a and 1b, respectively.  $F_0$  is the fluorescence intensity in the absence of quencher PQ or DQ at 336 nm or 416 nm.

**Table 6.** Association constants of H-G complexes at 25 °C, reported as logK. Paraquat, PQ, and diquat, DQ, are the guests, G, and the compounds 1a and 1b are the fluorescent hosts, H. The values were determined by Equation (3). Uncertainties are given as standard deviation.

Guest	Host	
	1a	1b
DQ	6.4 ± 0.2	6.8 ± 0.1
PQ	7.2 ± 0.1	7.3 ± 0.1

### 3.3. Fluorescent Detection of Paraquat and Diquat

The resulting emission spectra in the presence of paraquat or diquat show that the fluorescence is already quenched efficiently at  $\mu\text{g L}^{-1}$  concentrations of guest, and show a linear correlation between fluorescence change  $\Delta F = F_0 - F$  and the added guest concentration.  $F_0$  indicates the fluorescence intensity at  $[\text{PQ}] = 0 \mu\text{g L}^{-1}$  or  $[\text{DQ}] = 0 \mu\text{g L}^{-1}$  at 336 nm for naphthalene fluorophore 1a and at 416 nm for anthracene fluorophore 1b. In Figure 10, this adequate linearity at  $\mu\text{g L}^{-1}$  concentration is evident, indicating that the probes 1a and 1b can quantitatively detect these herbicides at ppb concentrations.

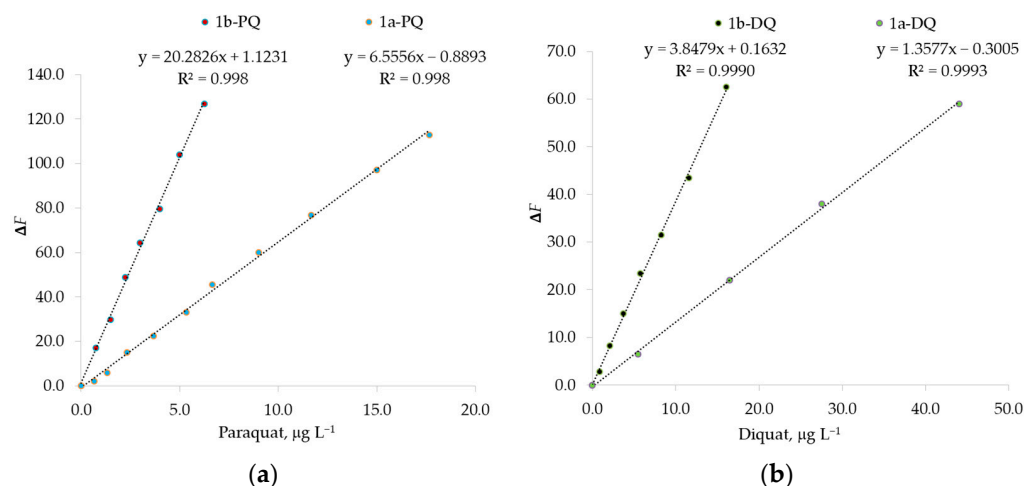


**Figure 10.** Fluorescence change  $\Delta F = F_0 - F$  of fluorophores 1a and 1b against (a) paraquat, PQ, or (b) diquat, DQ, concentrations in chloroform–methanol solution 1:1.  $F_0$  indicates the fluorescence at  $[\text{PQ}] = 0 \mu\text{g L}^{-1}$  or  $[\text{DQ}] = 0 \mu\text{g L}^{-1}$  at 336 nm for naphthalene fluorophore 1a and at 416 nm for anthracene fluorophore 1b.

To verify if it is possible to determine very low concentrations of these herbicides by fluorescent recognition, the detection limit was calculated from the fluorescence titration data, as defined by IUPAC [43,44]. The fluorescence spectra of fluorophores were measured ten times and the standard deviation of blank measurement was achieved at the prefixed wavelength. To gain the slope of the curve  $F$  against concentration, the fluorescence intensity data collected at the maximum were plotted against the concentration of paraquat or diquat. So, the detection limit was calculated with the following Equation (5):

$$\text{Detection limit} = 3 \sigma / m, \quad (5)$$

where  $\sigma$  is the standard deviation of blank measurement, and  $m$  is the slope of the linear equation that relates the maximum fluorescence intensity to the guest concentrations.

The calculated detection limits reported in Table 7 are comparable or better than those obtained with other sensors for determination of these analytes in water without sample pre-concentration [23,24]. The probes 1b-PQ and 1b-DQ present the best prospects for herbicide determination, especially the 1b-PQ probe, which was found to be the most sensitive under

the experimental conditions. Moreover, the calix-appended anthracene allows us to determine an herbicide concentration better than the calix-appended naphthalene fluorophore.

**Table 7.** Detection limits calculated for paraquat, PQ, and diquat, DQ, by fluorescence titration.

Guest	Host	<i>m</i>	Detection Limit, ng L <sup>-1</sup>	λ <sub>max</sub> , nm
DQ	1a	1.3577	464	336
DQ	1b	3.8479	164	416
PQ	1a	6.5556	96	336
PQ	1b	20.2826	31	416

For drinking water, the U.S. Environmental Protection Agency (EPA) has established a maximum contaminant level of 20 µg L<sup>-1</sup> for diquat and a desired goal of 3 µg L<sup>-1</sup> for paraquat (not EPA-regulated). The European Union has not regulated the levels of these compounds specifically in drinking water and continues to apply the value of 0.1 µg L<sup>-1</sup> expected for all pesticides [45,46]. Therefore, the proposed procedure method could be applied for the determination of these herbicides in water samples, by using hydroalcoholic solutions to allow host–guest solubility. However, it is also expected that the presence of the more polar solvent can play a significantly larger role in the electrostatic interactions and decrease or increase the fluorescence signal [47,48].

### 3.4. Validation of the Fluorescent Detection in Water Environment

A sample of tap water was spiked with different amounts of paraquat or diquat, ranging from 3 to 75 µg L<sup>-1</sup>, by using a standard solution of guest. All the samples were also treated with EDTA, 1 mg/mL, to suppress the possible interference of metal ions [49]. To avoid solvatochromic effects on fluorescence emission spectra [50], the method of standard additions was used [51], by adding methanol solutions of paraquat (or diquat) and 1b to several aliquots of the same volume of tap water, spiked at 1.0 µg L<sup>-1</sup> of total solution. The resulting hydroalcoholic solutions must have a concentration of 60% *v/v* in a compromise between signal peak height and adopting the highest concentration of water possible. Therefore, a concentration of sample water of 40% was selected for the experiments. Table 8 reports the experimental data for the paraquat test, plotted in Figure 11 as  $\Delta F = F_0 - F$ , in which the  $F_0$  value was measured in a non-spiked sample obtained from ultrapure, HPLC-grade water. The straight line intercepts the concentration axis at the expected value, in agreement with the extrapolated value of  $(1.1 \pm 0.2)$  µg L<sup>-1</sup> obtained from the standard addition method. It is evident that all species at a concentration normally found in tap water did not interfere (see Section 3.5). Similarly, a diquat test confirmed the spike concentration in the same sample of water used for the paraquat test. The experimental data for DQ test are gathered in Table 9 and Figure 12.

### 3.5. Tolerance Limit for Possible Interfering Species

As discussed, it seems evident that all species normally found in tap water did not interfere in the paraquat or diquat determination using a standard addition method. The detected species in our sample and their concentrations are reported in Table 10.

In this section, the effect of these water saline components was studied, but at a higher concentration to determine the tolerance concentration, defined as the concentration that did not vary by more than 5% for the analytical signal. Combining the salts NaCl, KNO<sub>3</sub>, Na<sub>2</sub>CO<sub>3</sub>, Na<sub>2</sub>SO<sub>4</sub>, Na<sub>3</sub>PO<sub>4</sub>, MgCl<sub>2</sub>, CaCO<sub>3</sub> and ZnSO<sub>4</sub>·7H<sub>2</sub>O, a sample of 10.0 mL of tap water was fortified 10× in these anions and cations and the difference in the maximum fluorescence intensity,  $F_0$ , was determined with respect to the  $F$  value recorded before the addition of these salts. The signal variation was calculated according to Equation (6):

$$\text{signal variation} = \frac{|F_0 - F|}{F_0}, \% \quad (6)$$

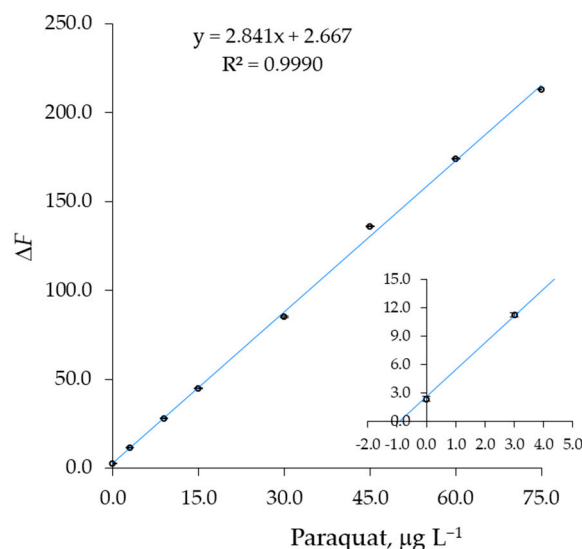


**Figure 11.** Standard additions plot obtained by adding a methanol solution of paraquat, PQ, and 1b to a tap water sample (3 replicates). The sample was divided into 8 equal aliquots. The spike concentration of  $1.0 \mu\text{g L}^{-1}$  was normalized to the total volume of solvent, 60/40 methanol/water. Inset: The straight line intersects the x-axis to the expected concentration of  $(1.1 \pm 0.1) \mu\text{g L}^{-1}$  of PQ.

**Table 8.** Experimental data for the standard additions plot reported in Figure 11.  $V_{1b}$  and  $V_{PQ}$  are the added volumes of the standard methanol solutions of  $[1b] = 2500 \mu\text{g L}^{-1}$  and  $[PQ] = 1500 \mu\text{g L}^{-1}$ , respectively. A tap water sample was spiked and divided into 8 aliquots. The spike concentration of  $1.0 \mu\text{g L}^{-1}$  was normalized to the total volume of  $2500 \mu\text{L}$ , 60/40 methanol/water.

Entry	$V_{\text{sample}}, \mu\text{L}$	$V_{1b}, \mu\text{L}$	$V_{PQ}, \mu\text{L}$	$V_{\text{TOT}}, \mu\text{L}$	$[1b], \mu\text{g L}^{-1}$	$[PQ], \mu\text{g L}^{-1}$	$\Delta F^*$
1	1000	25	0	2500	25.0	0.0	2.4
2	1000	25	5	2500	25.0	3.0	11.3
3	1000	25	15	2500	25.0	9.0	28.1
4	1000	25	25	2500	25.0	15.0	44.8
5	1000	25	50	2500	25.0	30.0	85.0
6	1000	25	75	2500	25.0	45.0	136.0
7	1000	25	100	2500	25.0	60.0	174.1
8	1000	25	125	2500	25.0	75.0	212.9

\* The fluorescence change  $\Delta F = F_0 - F$  was calculated with respect to the  $F_0$  value measured in a non-spiked water sample obtained as in entry 1, but from ultrapure, HPLC-grade water. The fluorescence values were measured at 416 nm for anthracene fluorophore 1b.  $\Delta F$  was calculated as an average value of three independent determinations.

**Table 9.** Experimental data for the standard additions plot reported in Figure 12.  $V_{1b}$  and  $V_{DQ}$  are the added volumes of the standard methanol solutions of  $[1b] = 2500 \mu\text{g L}^{-1}$  and  $[DQ] = 1500 \mu\text{g L}^{-1}$ , respectively. A tap water sample was spiked and divided into 8 aliquots. The spike concentration of  $1.0 \mu\text{g L}^{-1}$  was normalized to the total volume of  $2500 \mu\text{L}$ , 60/40 methanol/water.

Entry	$V_{\text{sample}}, \mu\text{L}$	$V_{1b}, \mu\text{L}$	$V_{DQ}, \mu\text{L}$	$V_{\text{TOT}}, \mu\text{L}$	$[1b], \mu\text{g L}^{-1}$	$[DQ], \mu\text{g L}^{-1}$	$\Delta F^*$
1	1000	25	0	2500	25.0	0.0	0.3
2	1000	25	5	2500	25.0	3.0	2.1
3	1000	25	15	2500	25.0	9.0	4.5
4	1000	25	25	2500	25.0	15.0	6.8
5	1000	25	50	2500	25.0	30.0	13.6
6	1000	25	75	2500	25.0	45.0	19.6
7	1000	25	100	2500	25.0	60.0	27.2
8	1000	25	125	2500	25.0	75.0	33.5

\* The fluorescence change  $\Delta F = F_0 - F$  was calculated with respect to the  $F_0$  value measured in a non-spiked water sample obtained as in entry 1, but from ultrapure, HPLC-grade water. The fluorescence values were measured at 416 nm for anthracene fluorophore 1b.  $\Delta F$  was calculated as the average value of three independent determinations.

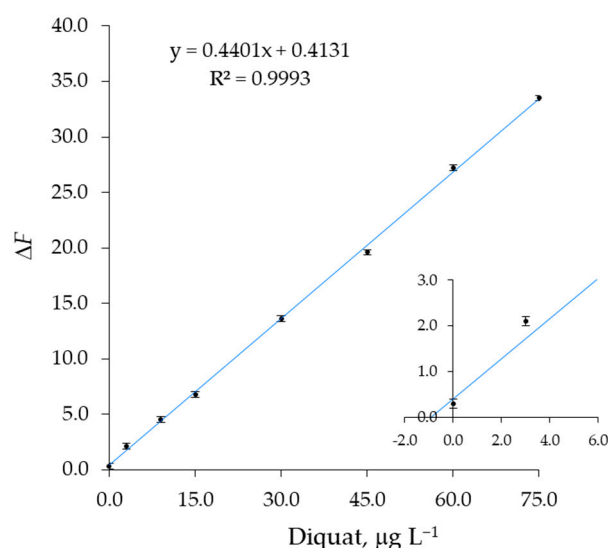


**Figure 12.** Standard additions plot obtained by adding a methanol solution of diquat, DQ, and 1b to a tap water sample (3 replicates). The sample was divided into 8 equal aliquots. The spike concentration of  $1.0 \mu\text{g L}^{-1}$  was normalized to the total volume of solvent, 60/40 methanol/water. Inset: The straight line intersects the x-axis to the value of  $(0.9 \pm 0.1) \mu\text{g L}^{-1}$  of diquat.

**Table 10.** Inorganic species detected in the tested sample of tap water and their effect on the determination of herbicide in a solution of these ions with a 10-fold higher concentration.

Species	Amount, $\text{mg L}^{-1}$ of Tested Sample	Addition <sup>1</sup> for 10.0 mL	Signal Variation, %
$\text{Ca}^{2+}$	42.1	10.52 mg, as $\text{CaCO}_3$	2
$\text{Mg}^{2+}$	12.3	4.89 mg, as $\text{MgCl}_2$	2
$\text{Zn}^{2+}$	0.8	0.35 mg, as $\text{ZnSO}_4 \cdot 7\text{H}_2\text{O}$	4
$\text{Na}^+$	39.4	0.70 mg, as $\text{NaCl}$ 3.23 mg, as $\text{Na}_2\text{SO}_4$ 0.03 mg, as $\text{Na}_3\text{PO}_4$ 6.03 mg, as $\text{Na}_2\text{CO}_3$	<1
$\text{K}^+$	3.1	0.81 mg, as $\text{KNO}_3$	<1
$\text{SO}_4^{2-}$	23.0	3.23 mg, as $\text{Na}_2\text{SO}_4$ 0.35 mg, as $\text{ZnSO}_4 \cdot 7\text{H}_2\text{O}$	3
$\text{PO}_4^{3-}$	0.2	0.03 mg, as $\text{Na}_3\text{PO}_4$	2
$\text{NO}_3^-$	5.0	0.81 mg, as $\text{KNO}_3$	4
$\text{CO}_3^{2-}$	98.0	10.52 mg, as $\text{CaCO}_3$ 6.03 mg, as $\text{Na}_2\text{CO}_3$	4
$\text{Cl}^-$	40.3	4.89 mg, as $\text{MgCl}_2$ 0.70 mg, as $\text{NaCl}$	3

<sup>1</sup> To evaluate the effect of the cations, EDTA was not added, also for solubility problems.

The addition did not produce any signal change greater than 5% at a herbicide concentration of  $1.0 \mu\text{g L}^{-1}$ . Instead, ion concentrations higher than 10 times can produce a signal variation depending on the concentration and the kind of species. Actually, the mineral content of typical tap or drinking water is within the tested range [52,53].

Potential cross-interferences were also evaluated by using Equation (6), comparing  $F_0$ , the maximum fluorescence intensity of a paraquat solution, with  $F$ , the maximum fluorescence intensity of an equimolar solution of paraquat and diquat. The last solution had the same concentration as the first solution, in the linear range from  $1.0$  to  $10.0 \mu\text{g L}^{-1}$ . At the same concentration of paraquat, no significant interferences were observed for DQ in this range (Table 11), probably because the interaction for the 1b-PQ probe is preferred

(Table 5). This probe also shows better calibration sensitivity with respect to the 1b-DQ probe (see Figure 10). Only when the diquat concentration is increased by more than 18 times with respect to the paraquat level, the variation in the fluorescence signal will be more than 5%. The most serious interference will be the presence of paraquat in the diquat direct determination, because of the higher affinity of 1a-1b hosts for PQ guest (Table 5). In this case, the PQ interference can be higher than 5%.

**Table 11.** Experimental data for the selectivity evaluation of the PQ-1b probe in the presence of diquat as interferent. The signal variation was calculated in the linear range from 1.0 to 10.0  $\mu\text{g L}^{-1}$  according to Equation (6), comparing  $F_0$ , the maximum fluorescence intensity of a paraquat solution, with  $F$ , the maximum fluorescence intensity of an equimolar solution of paraquat and diquat. The fluorescence values were measured at 416 nm for anthracene fluorophore 1b.

Entry	[1b], $\mu\text{g L}^{-1}$	[PQ], $\mu\text{g L}^{-1}$	$F_0$	[DQ], $\mu\text{g L}^{-1}$	$F$	Signal Variation, %
1	25.0	0.0	418.0	0.0	418.0	0.0
2	25.0	1.0	396.5	1.0	392.4	1.0
3	25.0	2.0	376.4	2.0	373.2	0.9
4	25.0	3.0	356.2	3.0	353.5	0.8
5	25.0	5.0	315.5	5.0	312.7	0.9
6	25.0	7.0	275.1	7.0	273.0	0.8
7	25.0	10.0	214.3	10.0	212.8	0.7

The standard addition method revisited can lead to adequate precision provided that a large excess of the analyte G was used and  $[G] > [H] > [\text{interferent guest}]$  [54,55]. Indeed, a large excess of the added guest G with respect to the interferent guest shifts the equilibrium towards the formation of host–guest favored by entropy. The result will be a distribution of points only slightly curved at low concentrations of G, when  $[G] < [H]$ . Instead, the calibration line achieved in the range  $[G] \geq [H]$  and extrapolated to zero signal provides a precise and accurate result. Experimental parameters, such as the increment size and the number of additions, must obviously be good enough to obtain a straight line (Table 12) [56].

**Table 12.** Experimental data for the evaluation of cross-interferences by using the standard addition method.  $V_{1b}$ ,  $V_{DQ}$  and  $V_{PQ}$  are the added volumes of the standard methanol solutions of [1b] = 2500  $\mu\text{g L}^{-1}$ , [DQ] = 3000  $\mu\text{g L}^{-1}$  and [PQ] = 1500  $\mu\text{g L}^{-1}$ , respectively.  $V_{PQ\text{-spike}}$  and  $V_{DQ\text{-spike}}$  are the volumes added to a tap water sample to spike it at the concentration of 6.0  $\mu\text{g L}^{-1}$ . This value was normalized to the total volume of 2500  $\mu\text{L}$ , 60/40 methanol/water. The sample was divided into 10 aliquots.

Entry	$V_{\text{sample}}$ , $\mu\text{L}$	$V_{1b}$ , $\mu\text{L}$	$V_{PQ\text{-spike}}$ , $\mu\text{L}$	$V_{DQ\text{-spike}}$ , $\mu\text{L}$	$V_{DQ}$ , $\mu\text{L}$	$V_{\text{TOT}}$ , $\mu\text{L}$	[1b], $\mu\text{g L}^{-1}$	[PQ] <sup>spike</sup> , $\mu\text{g L}^{-1}$	[DQ] <sup>spike</sup> , $\mu\text{g L}^{-1}$	[DQ], $\mu\text{g L}^{-1}$	$\Delta F$ *
0	1000	30	0	0	0	2500	30.0	0.0	0.0	0.0	0.0
1	1000	30	10	5	0	2500	30.0	6.0	6.0	0.0	17.9
2	1000	30	10	5	5	2500	30.0	6.0	6.0	6.0	18.2
3	1000	30	10	5	15	2500	30.0	6.0	6.0	18.0	19.2
4	1000	30	10	5	30	2500	30.0	6.0	6.0	36.0	21.9
5	1000	30	10	5	50	2500	30.0	6.0	6.0	60.0	29.1
6	1000	30	10	5	75	2500	30.0	6.0	6.0	90.0	41.9
7	1000	30	10	5	100	2500	30.0	6.0	6.0	120.0	55.6
8	1000	30	10	5	125	2500	30.0	6.0	6.0	150.0	68.4
9	1000	30	10	5	150	2500	30.0	6.0	6.0	180.0	81.7

\* The fluorescence change  $\Delta F = F_0 - F$  was calculated with respect to the  $F_0$  value measured in a non-spiked water sample obtained mixing the hydroalcoholic solution of 1b with ultrapure, HPLC-grade water (entry 0). The fluorescence values were measured at 416 nm for anthracene fluorophore 1b.

By plotting the  $\Delta F$  values reported in Table 12 against diquat concentration, [DQ], the intersection with the x-axis by extrapolation of the straight line obtained in the range

[DQ]  $\gg$  [1b] affords the expected diquat concentration of  $(6.1 \pm 0.3) \mu\text{g L}^{-1}$ , also in the presence of paraquat at the same concentration.

#### 4. Conclusions

In this work, a new fluorescent sensing method for paraquat and diquat was developed, and we focused on the improved determination of paraquat in tap and drinking waters. A calix[6]arene derivative containing anthracene or naphthalene as a pendant fluorophore at a lower rim can detect these herbicides in a very low concentration through the host–guest interaction. The fluorescence intensity change showed an adequate linear relationship with the herbicide concentrations. The linear response ranges were found from 1.0 to  $18 \mu\text{g L}^{-1}$  with the detection limit of  $31 \text{ ng L}^{-1}$ , and from 1.0 to  $44 \mu\text{g L}^{-1}$  with the detection limit of  $0.16 \mu\text{g L}^{-1}$  for paraquat and diquat, respectively.

**Author Contributions:** Conceptualization, T.C.; methodology, T.C. and F.S.; titration software, E.V.; validation, T.C.; formal analysis, T.C. and F.S.; investigation, T.C.; resources, T.C. and F.S.; data curation, T.C. and E.V.; writing—original draft preparation, T.C.; writing—review and editing, T.C. and E.V.; supervision, T.C.; project administration, T.C.; funding acquisition, T.C. All authors have read and agreed to the published version of the manuscript.

**Funding:** This research was funded by FATER S.p.A., Recover Project: CUP C27H18000110007, HORIZON 2020: Financing from the Axis I, Action Lines 1.1.1 E 1.1.4. POR FESR ABRUZZO 2014–2020.

**Institutional Review Board Statement:** Not applicable.

**Informed Consent Statement:** Not applicable.

**Data Availability Statement:** Not applicable.

**Acknowledgments:** We thank the research group of P. Neri (University of Salerno) for providing basic material.

**Conflicts of Interest:** The authors declare no conflict of interest.

#### References

1. Jones, G.M.; Vale, J.A. Mechanisms of toxicity, clinical features, and management of diquat poisoning: A review. *J. Toxicol. Clin. Toxicol.* **2000**, *38*, 123–128. [[CrossRef](#)] [[PubMed](#)]
2. Gupta, R.C.; Crismann, J.W. Agricultural Chemicals. In *Haschek and Rousseaux's Handbook of Toxicologic Pathology*, 3rd ed.; Haschek, W.M., Rousseaux, C.G., Wallig, M.A., Eds.; Academic Press: Boston, MA, USA, 2013; Volume 2, pp. 1349–1372.
3. World Health Organization. *The WHO Recommended Classification of Pesticides by Hazard and Guidelines to Classification 2009*; WHO: Geneva, Switzerland, 2009.
4. Code of Federal Regulation. *Restricted Use Products List, Pesticide Registration and Classification Procedures 40CFR*; Part 152.175; Office of Pesticide Programs (7510P), Environmental Protection Agency: Washington, DC, USA, 2022; Volume 40, Chapter I; pp. 54–65.
5. China Ministry of Agriculture Announcement No. 1745, 24 April 2012. Foodmate.net. Available online: <https://study.foodmate.net/web/dbk/detail?id=1378> (accessed on 27 November 2020).
6. European Commission. The Court of First Instance Annuls the Directive Authorising Paraquat as an Active Plant Protection Substance. Judgment of the Court of First Instance in Case T-229/04 Press Release No° 45/07 11 July 2007. Available online: <http://curia.europa.eu/jcms/upload/docs/application/pdf/2009-02/cp070045en.pdf> (accessed on 27 November 2020).
7. U.S. Environmental Protection Agency. *EPA Method 549.2. Determination of Paraquat of Diquat in Drinking Water by Liquid-Solid Extraction and High-Performance Chromatography with Ultraviolet Detection*; U.S. Environmental Protection Agency: Washington, DC, USA, 1997.
8. Otero, R.R.; Grande, B.C.; Perez-Lamela, C.; Simal-Gándara, J.; Arias-Estévez, M. Simultaneous determination of the herbicides diquat and paraquat in water. *J. Chromatogr. Sci.* **2006**, *44*, 539–542. [[CrossRef](#)]
9. Van Tran, K.; Shia, J.C.; Young, M.S. *Fast and Sensitive UPLC/MS Determination of Diquat and Paraquat in Drinking Water*; Waters Application Note No. 720004220en; Waters Corporation: Milford, MA, USA, 2012. Available online: <https://www.waters.com/webassets/cms/library/docs/720004220en.pdf> (accessed on 20 November 2015).
10. Ali, S.; Shah, M.R.; Hussain, S.; Khan, S.; Latif, A.; Ahmad, M.; Ali, M. A Facile Approach Based on Functionalized Silver Nanoparticles as a Chemosensor for the Detection of Paraquat. *J. Clust. Sci.* **2022**, *33*, 413–420. [[CrossRef](#)]
11. Sangsum, C.; Saetear, P. All-Step-in-One Test Kit for Paraquat Detection in Water and Vegetable Samples. *Analytica* **2022**, *3*, 92–105. [[CrossRef](#)]

12. Nunez, O.; Moyano, E.; Galcerán, M.T. Solid-phase extraction and sample stacking capillary electrophoresis for the determination of quaternary ammonium herbicides in drinking water. *J. Chromatogr. A* **2002**, *946*, 275–282. [[CrossRef](#)]
13. Zen, J.M.; Jeng, S.H.; Chen, H.J. Determination of paraquat by square-wave voltammetry at a perfluorosulfonated ionomer/clay-modified electrode. *Anal. Chem.* **1996**, *68*, 498–502. [[CrossRef](#)]
14. Paramalingam, T.; Yusoff, A.R.M.; Qureshi, M.S.; Shah, Z.A.; Sathishkumar, P.; Yusop, Z.; Khalid, M.; Khokhar, F.M. Determination of Paraquat Dichloride from Water Samples Using Differential Pulse Cathodic Stripping Voltammetry. *Russ. J. Electrochem.* **2018**, *54*, 1155–1163. [[CrossRef](#)]
15. Mastichiadis, C.; Kakabakos, S.E.; Christofidis, I.; Koupparis, M.A.; Willetts, C.; Misiakos, K. Simultaneous Determination of Pesticides Using a Four-Band Disposable Optical Capillary Immunosensor. *Anal. Chem.* **2002**, *74*, 6064–6072. [[CrossRef](#)]
16. Bacigalupo, M.A.; Meroni, G.; Mirasoli, M.; Parisi, D.; Longhi, R. Ultrasensitive Quantitative Determination of Paraquat: Application to River, Ground, and Drinking Water Analysis in an Agricultural Area. *J. Agric. Food Chem.* **2005**, *53*, 216–219. [[CrossRef](#)]
17. Wu, D.; Sedgwick, A.C.; Gunnlaugsson, T.; Akkaya, E.U.; Yoon, J.; James, T.D. Fluorescent chemosensors: The past, present, and future. *Chem. Soc. Rev.* **2017**, *46*, 7105–7123. [[CrossRef](#)]
18. Yoon, S.; Albers, A.E.; Wong, A.P.; Chang, C.J. Screening Mercury Levels in Fish with a Selective Fluorescent Chemosensor. *J. Am. Chem. Soc.* **2005**, *127*, 16030–16031. [[CrossRef](#)]
19. Yan, K.C.; Steinbrueck, A.; Sedgwick, A.C.; James, T.D. Fluorescent Chemosensors for Ion and Molecule Recognition: The Next Chapter. *Front. Sens.* **2021**, *2*, 731928. [[CrossRef](#)]
20. Chena, Z.; Álvarez-Pérez, M.; Villoslada, F.-N.; Moreno-Bondi, M.C.; Orellana, G. Fluorescent sensing of “quat” herbicides with a multifunctional pyrene-labeled monomer and molecular imprinting. *Sens. Actuators B Chem.* **2014**, *191*, 137–142. [[CrossRef](#)]
21. Zhao, Z.; Zhang, F.; Zhang, Z. A facile fluorescent “turn-off” method for sensing paraquat based on pyranine-paraquat interaction. *Spectrochim. Acta Part A Mol. Biomol. Spectrosc.* **2018**, *199*, 96–101. [[CrossRef](#)] [[PubMed](#)]
22. Kang, Z.; Yang, J.; Jiang, J.; Zhao, L.; Zhang, Y.; Tu, Q.; Wang, J.; Yuan, M.S. Pillar[5]arenes modified tetraphenylethylene as fluorescent chemosensor for paraquat detection. *Sens. Actuators B. Chem.* **2022**, *370*, 132436. [[CrossRef](#)]
23. Sun, S.; Li, F.; Liu, F.; Wang, J.; Peng, X. Fluorescence detecting of paraquat using host-guest chemistry with cucurbit[8]uril. *Sci. Rep.* **2014**, *4*, 3570. [[CrossRef](#)]
24. Ren, H.-X.; Mao, M.-X.; Li, M.; Zhang, C.-Z.; Peng, C.-F.; Xu, J.-G.; Wei, X.-L. A Fluorescent Detection for Paraquat Based on  $\beta$ -CDs-Enhanced Fluorescent Gold Nanoclusters. *Foods* **2021**, *10*, 1178. [[CrossRef](#)]
25. Talotta, C.; Caruso, T.; De Rosa, M.; Gaeta, C.; Soriente, A.; Neri, P. Threading fluorescent calixarene-wheels with ammonium axles. *Supramol. Chem.* **2018**, *30*, 627–641. [[CrossRef](#)]
26. Kim, J.S.; Quang, D.T. Calixarene-Derived Fluorescent Probes. *Chem. Rev.* **2007**, *107*, 3780–3799. [[CrossRef](#)]
27. Takahashi, M.; Tsuji, N.; Yazaki, K.; Sei, Y.; Obata, M. A fluorescent calix[4]arene with naphthalene units at the upper rim exhibits long fluorescence emission lifetime without fluorescence quenching. *RSC Adv.* **2021**, *11*, 11651–11654. [[CrossRef](#)] [[PubMed](#)]
28. Kumar, R.; Jung, Y.; Kim, J.S. Fluorescent Calixarene Hosts. In *Calixarenes and Beyond*; Neri, P., Sessler, J., Wang, M.X., Eds.; Springer: Cham, Switzerland, 2016; Chapter 28; pp. 743–760. [[CrossRef](#)]
29. Gaeta, C.; Talotta, C.; Margarucci, L.; Casapullo, A.; Neri, P. Through-the-Annulus Threading of the Larger Calix[8]arene Macrocycle. *J. Org. Chem.* **2013**, *78*, 7627–7638. [[CrossRef](#)] [[PubMed](#)]
30. Sauvage, J.P.; Dietrich-Buchecker, C. *Molecular Catenanes, Rotaxanes and Knots*; Wiley-VCH: Weinheim, Germany, 1999; pp. 143–163.
31. Stewart, D.R.; Gutsche, C.D. Isolation, Characterization, and Conformational Characteristics of *p*-tert-Butylcalix[9–20]arenes. *J. Am. Chem. Soc.* **1999**, *121*, 4136–4146. [[CrossRef](#)]
32. Del Valle, J.C.; Catalán, J. Kasha’s Rule: A Reappraisal. *Phys. Chem. Chem. Phys.* **2019**, *21*, 10061–10069. [[CrossRef](#)] [[PubMed](#)]
33. De Caro, C.; Aichert, A. *Water Determination by Karl Fischer Titration, Metrohm Application Bulletin 407/1e*; Metrohm Ltd.: Herisau, Switzerland, 2017; pp. 1–4.
34. Friedel, R.A.; Orchan, M. *UltraViolet Spectra of Aromatic Compounds*; Wiley: London, UK; Chapman & Hall: New York, NY, USA, 1951.
35. Lakowicz, J.R. *Principles of Fluorescence Spectroscopy*, 3rd ed.; Kluwer Academic Plenum Publisher: New York, NY, USA, 2006; Chapter 8; pp. 243–245, 278–330.
36. Benesi, H.; Hildebrand, J. A Spectrophotometric Investigation of the Interaction of Iodine with Aromatic Hydrocarbons. *J. Am. Chem. Soc.* **1949**, *71*, 2703–2707. [[CrossRef](#)]
37. Liu, Y.; Han, B.-H.; Sun, S.-X.; Wada, T.; Inoue, Y. Molecular Recognition Study on Supramolecular Systems. 20. Molecular Recognition and Enantioselectivity of Aliphatic Alcohols by L-Tryptophan-Modified beta-Cyclodextrin. *J. Org. Chem.* **1999**, *64*, 1487–1493. [[CrossRef](#)]
38. Peluso, A.; Caruso, T.; Landi, A.; Capobianco, A. The Dynamics of Hole Transfer in DNA. *Molecules* **2019**, *24*, 4044. [[CrossRef](#)] [[PubMed](#)]
39. Thordarson, P. Determining association constants from titration experiments in supramolecular chemistry. *Chem. Soc. Rev.* **2011**, *40*, 1305–1323. [[CrossRef](#)]
40. Castanho, M.A.R.B.; Prieto, M.J.E. Fluorescence quenching data interpretation in biological systems. The use of microscopic models for data analysis and interpretation of complex systems. *Biochim. Biophys. Acta-Biomembr.* **1998**, *1373*, 1–16. [[CrossRef](#)]
41. Kohlmann, T.; Goetz, M. Combined static and dynamic intracellular fluorescence quenching: Effects on stationary and time-resolved Stern–Volmer experiments. *Phys. Chem. Chem. Phys.* **2019**, *21*, 10075–10085. [[CrossRef](#)]

42. Genovese, D.; Cingolani, M.; Rampazzo, E.; Prodi, L.; Zaccheroni, N. Static quenching upon adduct formation: A treatment without shortcuts and approximations. *Chem. Soc. Rev.* **2021**, *50*, 8414–8427. [[CrossRef](#)]
43. Long, G.L.; Winefordner, J.D. Limit of Detection: A Closer Look at the IUPAC Definition. *Anal. Chem.* **1983**, *55*, 712A–724A. [[CrossRef](#)]
44. Li, Y.; Zhang, X.; Zhu, B.; Yan, J.; Xu, W. A highly selective colorimetric and "off-on-off" fluorescent probe. *Anal. Sci.* **2010**, *26*, 1077–1080. [[CrossRef](#)]
45. Commission of the European Communities. Drinking Water Guideline 80/778/EEC, No. L229/11-29, Brussels. 1980. Available online: <https://op.europa.eu/en/publication-detail/-/publication/c0f580d3-a6a6-4164-a27c-587ce0ec2ea8/language-en/format-PDF/source-search> (accessed on 15 July 1980).
46. European Environment Agency. Directive 2000/60/EC of the European Parliament and of the Council of 23 October 2000 Establishing a Framework for Community Action in the Field of Water Policy. *Off. J. Eur. Communities Legis.* **2000**, *43*, L327.
47. Reichardt, C. *Solvents and Solvent Effects in Organic Chemistry*, 3rd ed.; Wiley VCH: Weinheim, Germany, 2003; pp. 352–358.
48. Schönbeck, C.; Li, H.; Han, B.-H.; Laursen, B.V. Solvent effects and driving forces in pillararene inclusion complexes. *J. Phys. Chem. B* **2015**, *119*, 6711–6720. [[CrossRef](#)] [[PubMed](#)]
49. Maya, F.; Estela, J.M.; Cerda, V. Improved spectrophotometric determination of PQ in drinking waters exploiting a Multisyringe liquid core waveguide system. *Talanta* **2011**, *85*, 588–595. [[CrossRef](#)]
50. Nigam, S.; Rutan, S. Principles and Applications of Solvatochromism. *Appl. Spectrosc.* **2001**, *55*, 362–370A. [[CrossRef](#)]
51. U.S. Environmental Protection Agency. *EPA Method 600/4-79/020; Methods for Chemical Analysis of Water and Wastes*. U.S. Environmental Protection Agency: Washington, DC, USA, 1983.
52. Patterson, K.K.; Pehrsson, P.R.; Perry, C.R. The mineral content of tap water in United States households. *J. Food Compos. Anal.* **2013**, *31*, 46–50. [[CrossRef](#)]
53. Wetzel, R.G. Salinity of Inland Waters. In *Limnology*, 3rd ed.; Wetzel, R.G., Ed.; Academic Press: San Diego, CA, USA, 2001; p. 170.
54. Andersen, J.E.T. The standard addition method revisited. *Trends Anal. Chem.* **2017**, *89*, 21–33. [[CrossRef](#)]
55. Wiczorek, M.; De Bosz, M.; Swit, P.; Piech, A.; Koscielniak, P. Reliable calibration by nonlinear standard addition method in the presence of additive interference effects. *Chem. Mon.* **2018**, *149*, 1567–1572. [[CrossRef](#)]
56. Koscielniak, P. Nonlinear calibration by the standard addition method. *Chemom. Intell. Lab. Syst.* **1999**, *47*, 275–287. [[CrossRef](#)]

**Disclaimer/Publisher's Note:** The statements, opinions and data contained in all publications are solely those of the individual author(s) and contributor(s) and not of MDPI and/or the editor(s). MDPI and/or the editor(s) disclaim responsibility for any injury to people or property resulting from any ideas, methods, instructions or products referred to in the content.